Article

Performance Analysis of a Waste-to-Energy System Integrated with the Steam–Water Cycle and Urea Hydrolysis Process of a Coal-Fired Power Unit

Yuanyuan Zhang [1], Lai Wei [1], Xin Gao [1], Heng Chen [1,*], Qiubai Li [2], Kai Zhang [1] and Qilong Huang [2]

[1] Beijing Key Laboratory of Emission Surveillance and Control for Thermal Power Generation, North China Electric Power University, Beijing 102206, China; 51101894@ncepu.edu.cn (Y.Z.); l.wei@ncepu.edu.cn (L.W.); supper1234567890@126.com (X.G.); kzhang@ncepu.edu.cn (K.Z.)

[2] State Key Laboratory of Clean and Efficient Coal-Fired Power Generation and Pollution Control, China Energy Science and Technology Research Institute Co., Ltd., Nanjing 210023, China; qiubai.li@chnenergy.com.cn (Q.L.); huangqilong0451@163.com (Q.H.)

* Correspondence: heng@ncepu.edu.cn; Tel.: +86-(10)-6177-2284

Abstract: An innovative hybrid energy system consisting of a waste-to-energy unit and a coal-fired power unit is designed to enhance the energy recovery of waste and decrease the investment costs of waste-to-energy unit. In this integrated design, partial cold reheat steam of the coal-fired unit is heated by the waste-to-energy boiler's superheater. The heat required for partial preheated air of waste-to-energy unit and its feedwater are supplied by the feedwater of CFPU. In addition, an additional evaporator is deployed in the waste-to-energy boiler, of which the outlet stream is utilized to provide the heat source for the urea hydrolysis unit of coal-fired power plant. The stand-alone and proposed designs are analyzed and compared through thermodynamic and economic methods. Results indicate that the net total energy efficiency increases from 41.84% to 42.12%, and the net total exergy efficiency rises from 41.19% to 41.46% after system integration. Moreover, the energy efficiency and exergy efficiency of waste-to-energy system are enhanced by 10.48% and 9.92%, respectively. The dynamic payback period of new waste-to-energy system is cut down from 11.39 years to 5.48 years, and an additional net present value of $14.42 million is got than before.

Keywords: waste-to-energy unit; coal-fired power unit; feedwater heating; urea hydrolysis; integrated power generation system

1. Introduction

With the development of economy and society, the urbanization process has accelerated and residents' living standards have been improved in China. Yet municipal solid waste management (MSWM) has become a pronounced problem because of the population concentration and increased consumption during urbanization [1]. More than one-third of the cities and towns have fallen into the predicament of garbage siege and have been surrounded by landfills [2], which seriously hinders the sustainable development of society. During the 10 years from 2010 to 2019, the volume of municipal solid waste (MSW) removal rose from 158 million tons a year to 242 million tons a year in China [3]. Besides, population explosion and rapid urbanization have also brought about the rapid growth of MSW in urban areas worldwide. Global MSW may increase by 0.9 billion tons from 2010 to 2025 [4]. In particular, the urban population of East Asia and Pacific region is much higher than other regions, and the per capita MSW production rate could increase by 60% from 2012 to 2025 [5]. The garbage growth rate is commonly higher than the urbanization rate, and the garbage is piled up around cities and towns, causing environmental pollution and landscape deterioration. Consequently, appropriate MSWM is an urgent and vital task in China and critical to the world's sustainable development.

MSWM includes biological treatment and chemical treatment methods, of which biological treatment technologies cover landfilling, digestion and composting and chemical treatment technologies comprise incineration, gasification and pyrolysis. Nevertheless, to date, landfilling and incineration are still the prime methods in most countries [6]. Several reasons can be summarized: One is that a part of biological treatment technologies take a long time and there are many problems to be solved [7]; another is that most developing countries take economy and technology into account, and they still prefer landfilling when land resources are available [8]; the last is that waste incineration plants occupy small area and recover energy while reducing waste, which is better than other waste treatment methods [9]. According to the changes in the number of the newly added MSW harmless treatment plants in China from 2015 to 2019 [3], the proportion of MSW incineration plants has increased rapidly in the total MSW treatment plants while the number of MSW landfills no longer augments after 2015. Cities have been surrounded by landfills and improper filtrate treatment issues occur in them, which can partly explain the upsurge of MSW incineration treatment plants in China [2,10]. Moreover, since fossil fuels account for a relatively high proportion of the global primary energy, waste incineration technology not only treats a large amount of waste but also recovers its energy to offset part of the consumption of fossil fuels [11].

However, compared with conventional coal-fired power units (CFPUs), the energy efficiency of waste-to-energy units (WTEUs) is lower due to lower steam parameters, higher condensing pressure, higher auxiliary power consumption rate and more exhaust flue gas energy loss. The current behaviors to enhance the energy efficiency of WTEUs mainly focus on raising steam parameters and utilizing exhaust flue gas heat. The live steam temperature and pressure in waste-to-energy (WTE) boilers are usually designed at 400 °C and 40 bar, respectively [12]. Raising steam parameters can recover more energy of MSW and enhance power efficiency, while the high-temperature flue gas produced by MSW incineration could cause high-temperature corrosion of heat exchangers in WTE boilers [13,14]. Xu et al. [4] introduced a new type of refractory brick to the combustion chamber, which delivers more heat, allows steam to superheat on waterwall, reduces corrosion risks and increases the WTEU efficiency. Martin et al. [15] arranged an anti-corrosion radiation superheater (SH) in the high-temperature flue gas area to achieve higher steam temperature. Ralf Koralewska [16] divided the flue gas above the grate into two parts with different chlorine concentrations and used the low-corrosive part to heat SH for higher steam temperature. Bogale et al. [17] combine the external superheating of live steam with the reheating of exhaust steam from a high-pressure turbine, upgrading the live steam parameters and the reheat steam parameters.

Additionally, many experts have tried to decline the energy loss of exhaust flue gas. Liuzzo et al. [18] utilized flue gas recirculation to limit the temperature of combustion chamber, reducing pollutants in the flue gas and decreasing its mass flow. Less excess air could reduce flue gas mass flow too, but it is necessary to pay attention to maintain combustion stability [19]. Oxygen-enriched air was consumed by Martin et al. [15] to diminish flue gas mass flow due to the reduction of the air entering furnace. Considering the complex chemical composition of exhaust flue gas, its temperature is usually higher than that of other power plants and it seriously affects the energy efficiency of WTE plants. Therefore, many researchers have presented strategies for waste heat recovery. It was suggested to exploit available low-temperature streams in WTE plants to preheat air or water to gain higher energy efficiency of heat recovery system [20]. Lombardi et al. [12] proposed using the water in the grate cooling circuit to preheat air. It is a relatively simple way to directly heat feedwater with the flue gas waste heat [21]. Similarly, employing flue gas waste heat for district heating is also recognized [22]. Nonetheless, people would face low-temperature corrosion issues while utilizing the flue gas waste heat [23]. On account of this, it may be inevitable to eliminate the corrosive constituents of exhaust flue gas before recovering waste heat, but associated equipment is complicated and expensive [24]. Besides the mentioned ways, the efficiency of WTE plants would also be influenced by the mode of

production. Many scholars have proved that combined heat and power (CHP) production could enhance power plants' energy efficiency [25,26], while power generation might be the only energy output option under the unavailability of district network heating [27]. In addition, researchers augmented power efficiency by combining the WTE system with other energy systems [20]. Arabkoohsar et al. [22] connected CHP with the Organic Rankine Cycle (ORC) based on a WTE system and drew on flue gas to provide high-temperature heat for ORC. An absorption refrigeration system was incorporated into the CHP of a WTE plant to form a combined cooling, heat and power (CCHP) system, optimizing the WTE efficiency [28]. Bianchi et al. [29] investigated the WTE systems coupled with gas combined cycles, and results demonstrated that the hybrid system could obtain higher net power efficiency and economic benefits than the separate system. A combination of a WTE plant and solar energy facilities was studied, using solar energy to attain external superheating and achieving a 4.5% net efficiency enhancement [30]. Chen et al. [31] combined a WTEU and a CFPU, upgrading total power efficiency and getting economic profits.

Due to the massive number of CFPUs in China, under this circumstance, research on the integration with coal-fired generating units are of great significance. The higher efficiency and greater stability of coal-fired units enable better use of the energy entering them, especially from lower energy efficiency power plants, such as WTE plants. Scholars have explored different coupling methods of a WTEU and a CFPU. However, few studies have incorporated the auxiliary devices of CFPUs into system integration. According to the national control standards for flue gas pollutants, the concentration of flue gas pollutants emitted directly after coal combustion exceeds the standard. Selective catalytic reduction (SCR) reactors are arranged in the tail flue of many power plant boilers to remove the nitrogen oxides (NO_x) in flue gas. The SCR method is widely used in power plant boilers. It sprays the ammonia diluted to a specific concentration into the flue gas. Under the action of catalysts, NO_x is reduced to nitrogen and water. The designed reducing agent used in most power plants is liquid ammonia. However, domestic relevant departments have stipulated that if the storage capacity of ammonia exceeds 10 tons, it would be defined as a hazard installation. Additionally, most CFPUs apply liquid ammonia as a reducing agent in SCR reactor, and the storage capacity of liquid ammonia is generally designed to meet the requirements of 5 to 7 days of 100% load, which is more than 10 tons [32]. Therefore, the ammonia production area of CFPUs is commonly regarded as a hazard installation. According to the requests of related policies and regulations, the denitration reductant is changed from liquid ammonia to urea to eliminate the risks of transportation and storage of liquid ammonia. It is foreseeable that many CFPUs would apply urea to produce ammonia instead of using liquid ammonia. The urea hydrolysis process could eradicate the potential danger caused by storage and transportation of liquid ammonia and have technical advantages of centralized layout, stability and reliability, which makes it an ideal technology to replace liquid ammonia. The medium pressure and high-temperature steam of boilers is usually used as the heat source for hydrolysis reaction in the urea hydrolyzer of coal-fired power plant. The steam quality is high, and its exergy loss as the external heating source is severe. Before entering the hydrolyzer, the steam needs to be cooled and depressurized by spraying demineralized water. While increasing the consumption of demineralized water, it also causes the fluctuation of the operation of the hydrolysis unit, which affects the production of ammonia gas. When coupling different thermal systems, it is necessary to consider the coupling scheme in detail to maximize the power generation. In particular, when integrating coal-fired power plants with other power plants, due to the complexity of coal-fired power systems, the arrangement of their energy-consuming auxiliary equipment needs to be thought, taking the layout of urea hydrolysis unit (UHU) as an example in this article.

This study develops a deep integration of a 500 t/d WTEU and a 660 MW CFPU based on the steam–water cycle and hydrolysis of urea into ammonia process, according to the existing research on the integration of a waste incineration plant and a coal-fired power plant [31,33]. The performance of this integrated design is evaluated by thermo-

dynamic analysis and economic analysis methods, which is described by the previous works [25,34,35]. In the hybrid system, the energy produced by waste incineration is delivered to the CFPU, which dramatically increases the power output of WTE system. The chief goals and innovations of this work could be concluded as follows: (1) Establish a novel integrated WTE system based on urea hydrolysis process and optimized steam–water cycle. (2) Transfer the heat source of UHU to the WTE system to reduce energy consumption and to improve UHU security and flexibility. (3) Deliver the energy of MSW to the steam–water cycle of CFPU. (4) Examine the advantages of the integrated system through thermodynamic and economic analysis methods. (5) Discuss the net power output of different integrated modes.

2. Methodology

Based on the previous research on the integration of WTEU and CFPU systems [31,33], this article further optimized the integrated design and proposed the layout of auxiliary devices in the system integration. The two power plants mentioned in this article are in operation. EBSILON Professional Version 13.02 (a product of STEAG Energy Services) is employed to integrate different thermal systems, which is widely used in the design, optimization, transformation, and operation of power plant thermal systems [36]. Through the built-in modules of EBSILON Professional, the models of stand-alone designs are built, and their simulation data are compared with their design data. Then the model of combined design is established after the data validation of simulation and design of the stand-alone systems. Finally, the initial and integrated systems' energy, exergy and economy are analyzed and compared.

3. System Description

3.1. Reference Waste-to-Energy Unit

The WTEU locates in eastern China, which operates continuously 24 h a day, and its annual operating hour is not less than 7000 h. It equips with a 500 t/d mechanical grate incinerator and a 10 MW condensing steam turbine generator set and is depicted in Figure 1. The feed fuel is MSW, including household garbage and urban road cleaning garbage. The composition of MSW and the main operating parameters of WTEU are recorded in Tables 1 and 2, respectively. The flue gas in combustion chamber needs to be kept above 850 °C for more than two seconds to inhibit the production of dioxins and other harmful substances [37]. Then flue gas flows through each heat exchanger to heat feedwater or steam. At last, cleaning devices would treat exhaust flue gas. However, the exhaust flue gas temperature behind ECO should not be too low because of the possible low-temperature corrosion caused by complex flue gas composition. Hence, the exhaust flue gas temperature generally demands more than 190 °C. High exhaust flue gas temperature would cause large energy loss and decrease the boiler's thermal efficiency. Besides, because of low live steam parameters, high exhaust steam parameters and high auxiliary power rate, the net power generation efficiency of reference WTEU is less than 20%.

In the WTEU, a regenerative heating system consisting of two regenerative heaters (RHs) is adopted to raise the feedwater temperature of WTE boiler. To intensify the waste combustion in WTE boiler, the air involved in the ignition and combustion of waste is preheated by the extraction steam from boiler drum and steam turbine (ST). The significant parameters of air preheaters (APHs) are displayed in Table 3. The APHs comprise a primary air heater (PAH) and a secondary air heater (SAH). The PAH is split into three sections, and the first section of PAH (PAH1) connects with the third section of PAH (PAH3). The boiler drum provides the saturated steam for PAH3 to heat the outlet air, and the condensate from PAH3 flows into PAH1 to heat the inlet air. The ST's first stage extraction steam supplies heat to the second section of PAH (PAH2) and the SAH. The primary air is heated from 15.0 °C to 220.0 °C in PAH, and the secondary air temperature is enhanced from 15.0 °C to 166.0 °C in SAH. A larger logarithmic mean temperature difference (LMTD) could decrease the area of APHs while it might cause greater exergy destruction in such components.

Figure 1. Diagram of the reference WTEU.

Table 1. Properties of the fuel used by WTEU (as received basis).

Fuel	Proximate Analysis (wt%)			Ultimate Analysis (wt%)						LHV (kJ/kg)
	A	M	C	H	O	N	S	Cl		
MSW	41.75	20.59	21.97	1.91	12.78	1.91	0.20	0.30		7000

A: ash; M: moisture; LHV: lower heating value.

Table 2. Operating parameters of the WTEU.

Parameter		Unit	Value
Fuel consumption rate (MSW)		kg/s	5.79
Live steam	Pressure	MPa	4.10
	Temperature	°C	400
	Mass flow	kg/s	13.50
Exhaust steam	Pressure	MPa	0.007
	Temperature	°C	39.0
	Mass flow	kg/s	9.95
Boiler efficiency		%	78.55
Total power generation		MW	9.75
Net power generation		MW	8.00
Net WTE efficiency		%	19.73

Table 3. Parameters of the APHs in WTEU.

	Parameter	Unit	PAH1	PAH2	PAH3	SAH
Cold side	Inlet/outlet fluid	-	Air/air	Air/air	Air/air	Air/air
	Inlet/outlet temperature	°C	15.0/31.1	31.1/166.0	166.0/220.0	15.0/166.0
	Mass flow	kg/s	20.48	20.48	20.48	8.38
Hot side	Inlet/outlet fluid	-	Condensate/ condensate	Steam/ condensate	Steam/ condensate	Steam/ condensate
	Inlet/outlet pressure	MPa	4.30/3.90	1.31/1.30	4.50/4.30	1.31/1.30
	Inlet/outlet temperature	°C	224.1/101.0	290.7/102.5	257.4/224.1	290.7/102.3
	Mass flow	kg/s	0.62	1.08	0.62	0.49
	LMTD	°C	132.4	95.6	47.0	104.9
	Heat load	MW	0.33	2.79	1.13	1.28

3.2. Reference Coal-Fired Power Unit

The CFPU locates in northern China, which adopts one supercritical parameter and variable pressure operation boiler. The sketch map of the selected 660 MW CFPU is described in Figure 2. The steam turbine generator set comprises one high-pressure steam turbine (HPST), one intermediate-pressure steam turbine (IPST), two low-pressure steam turbines (LPSTs) and one electricity generator (EG). The regenerative steam extraction system employs eight RHs to heat feedwater (RH1-8), and the extraction steam and feedwater parameters are depicted in Table 4. The main operating parameters of CFPU are given in Tables 5 and 6, respectively. Due to the relatively higher parameters of steam from SH outlet and reheater (RHR) outlet and the comparatively complete steam–water cycle, the net power efficiency of CFPU could reach 42.44%, which is far higher than that of WTE plants.
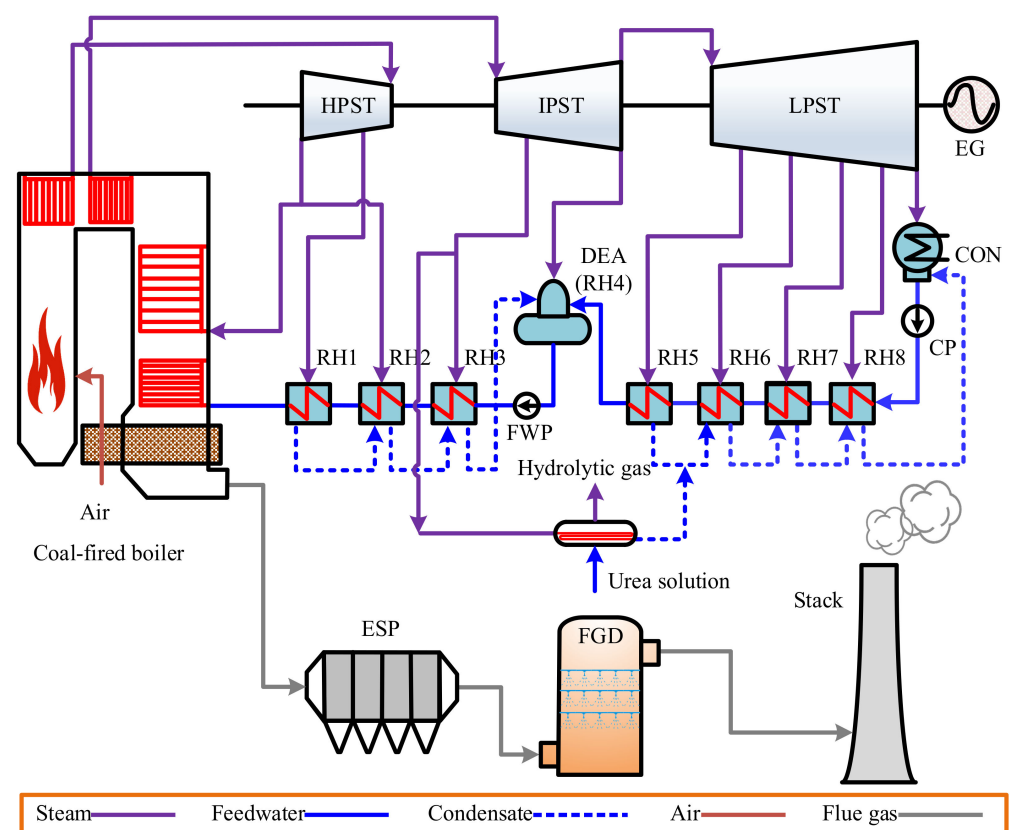

Figure 2. Diagram of the reference CFPU.

Table 4. Parameters of the regenerative steam extraction system of CFPU.

	Parameter	Unit	RH1	RH2	RH3	RH4	RH5	RH6	RH7	RH8
Extracted steam	Pressure	MPa	5.81	4.11	2.02	1.01	0.39	0.13	0.06	0.02
	Temperature	°C	352.5	316.2	473.3	359.4	253.1	136.8	86.7	61.0
	Mass flow	kg/s	28.53	40.49	19.74	26.43	24.04	12.76	16.09	15.20
Feedwater	Inlet/outlet temperature	°C	252.0/ 275.2	213.0/ 252.0	185.9/ 213.0	140.0/ 180.2	103.7/ 140.0	83.9/ 103.7	58.2/ 83.9	33.3/ 58.2
	Outlet mass flow	kg/s	506.35	506.35	506.35	506.35	391.16	391.16	391.16	391.16
Drain water	Temperature	°C	257.5	218.6	191.4	-	109.2	89.4	63.8	38.9
	Mass flow	kg/s	28.53	69.02	88.76	-	24.04	37.38	53.47	68.67

Table 5. Properties of the fuel used by CFPU (as received basis).

Fuel	Proximate Analysis (wt%)			Ultimate Analysis (wt%)					LHV (kJ/kg)
	A	M	C	H	O	N	S		
Coal	19.70	6.00	67.60	2.70	1.80	0.90	1.30		24,720

A: ash; M: moisture; LHV: lower heating value.

Table 6. Major parameters of the CFPU.

Parameter		Unit	Value
Fuel consumption rate (coal)		kg/s	59.72
ECO	Inlet fluid	-	Feedwater
	Inlet pressure	MPa	29.30
	Inlet temperature	°C	275.2
	Mass flow	kg/s	506.35
SH	Outlet fluid	-	Superheated steam
	Outlet pressure	MPa	24.20
	Outlet temperature	°C	566.0
	Mass flow	kg/s	506.35
RHR	Inlet/outlet pressure	MPa	4.24/3.82
	Inlet/outlet temperature	°C	308.4/566.0
	Mass flow	kg/s	432.31
Exhaust gas temperature		°C	122.0
Total power generation		MW	659.57
Net power generation		MW	626.59
Boiler efficiency		%	93.22
Net power efficiency		%	42.44

The reductant provided for the SCR denitration reactor of CFPU boiler is the ammonia produced by urea hydrolysis, and ammonia is a suitable reactant widely used in power plants to remove NO_x in the flue gas. The inlet flue gas volume of the SCR denitration device is 2,200,000 Nm^3/h in this power unit, and the inlet NO_x concentration is approximately 900 $mg/(Nm^3)$. The NO_x removal rate of SCR reactor exceeds 90%, and its outlet NO_x concentration is calculated as 40 $mg/(Nm^3)$. The mass flow of the consumed urea is calculated according to the following formulas [38]. The mass concentration of urea solution entering the hydrolysis device is 50%. The saturated steam at 180 °C is used for urea hydrolyzing in UHU, and the operating temperature of UHU is controlled at 150 °C. Moreover, catalysts can be added to accelerate reaction velocity based on the conventional urea hydrolysis process and improve the operational flexibility of device. Sun et al. [32] estimated the necessary heat of the urea hydrolysis process. According to the theoretical

calculation, the designed urea mass for the operation of CFPU should not be less than 1.21 t/h. The results obtained by theoretical calculations are described in Table 7.

$$\Delta Q_{NO_X} = \frac{M_{NO}}{M_{NO_2}} (NO_{X,in} - NO_{X,out}) \tag{1}$$

$$m_{NH_3} = \frac{n \times \Delta Q_{NO_X} \times V \times M_{NH_3}}{M_{NO} \times 10^6 \times \eta} \tag{2}$$

$$m_{CO(NH_2)_2} = \frac{m_{NH_3} \times M_{CO(NH_2)_2}}{2 \times M_{NH_3}} \tag{3}$$

where ΔQ_{NO_X} is the amount of removed NO_x, mg/m^3; m_{NH_3} is the mass flow of NH_3, kg/h; $m_{CO(NH_2)_2}$ is the mass flow of urea, kg/h; n is the mole ratio of NH_3 to NO_x, taking 0.96; V is the inlet flue gas volume of SCR denitration device, m^3/h; M_{NO}, M_{NO_2}, M_{NH_3} and $M_{CO(NH_2)_2}$ are the molar masses of NO, NO_2, NH_3 and $CO(NH_2)_2$, respectively; η is the volume fraction of the NO in NO_x, taking 99% [39].

Table 7. Parameters of the UHU of CFPU.

	Parameter	Unit	Value
Cold side	Inlet/outlet fluid	-	Urea solution/ Hydrolytic gas
	Inlet/outlet temperature	°C	50.0/150.0
	Mass flow	kg/s	0.67
Hot side	steam pressure	MPa	2.13
	steam temperature	°C	473.9
	steam flow	kg/s	0.58
	Attempering water pressure	MPa	1.10
	Attempering water temperature	°C	25.0
	Attempering water flow	kg/s	0.14
	LMTD	°C	76.9
	Heat load	MW	1.41

However, the heating steam source used during the operation of urea hydrolyzer is high-temperature superheated steam (the third stage extraction steam of steam turbines). The extraction steam is of high quality and is wasted seriously as an external heating source. It needs to be sprayed demineralized water to cool down and reduce pressure before entering the hydrolyzer. It increases the consumption of demineralized water and causes fluctuations in the operation of hydrolyzer, resulting in changes in the amount of ammonia produced by the hydrolyzer, and at the same time, affecting the removal of NO_x.

3.3. Proposed Integrated Design

A conceptual scheme is proposed to combine the WTEU and the CFPU to use the energy from MSW, as illustrated in Figure 3. In this integrated design, most of the energy generated by MSW incineration is transferred to the steam–water system of CFPU, increasing total power generation significantly. The followings are the description of the connection between WTEU and CFPU.

1. Remove ST, EG, RHs and condenser (CON) of the WTEU. Both WTEU and CFPU use the steam turbine generator set of CFPU for electricity generation.
2. The saturated steam of WTE boiler drum is transported to the second stage extraction steam to heat the feedwater flowing into the RH2.
3. The SH of WTEU no longer heats the saturated steam from boiler drum but heat partial exhaust steam from the HPST of CFPU. Then the steam from the SH outlet of WTE boiler returns to the reheater of coal-fired boiler for further heat absorption.

4. Since the steam employed in the original urea hydrolyzer derives from the third stage extraction steam of STs of CFPU, decreasing the work output and efficiency of STs. An additional evaporator (AE) is deployed in the ECO space of WTE boiler to supply the heating steam to the urea solution hydrolysis.

5. The fluid entering the ECO of WTEU is the feedwater from the DEA outlet of CFPU, and the fluid getting into AE extracts from the feedwater of the suggested WTE system.

6. The heat source of PAH2 and SAH is changed from the first stage extraction steam of ST of original WTEU to the feedwater from DEA outlet of CFPU, while the heat source of PAH3 and PAH1 remains unchanged. Then the cooling water from PAH1, PAH2 and SAH gathers and flows into the CON of CFPU with the drain water of RH8.
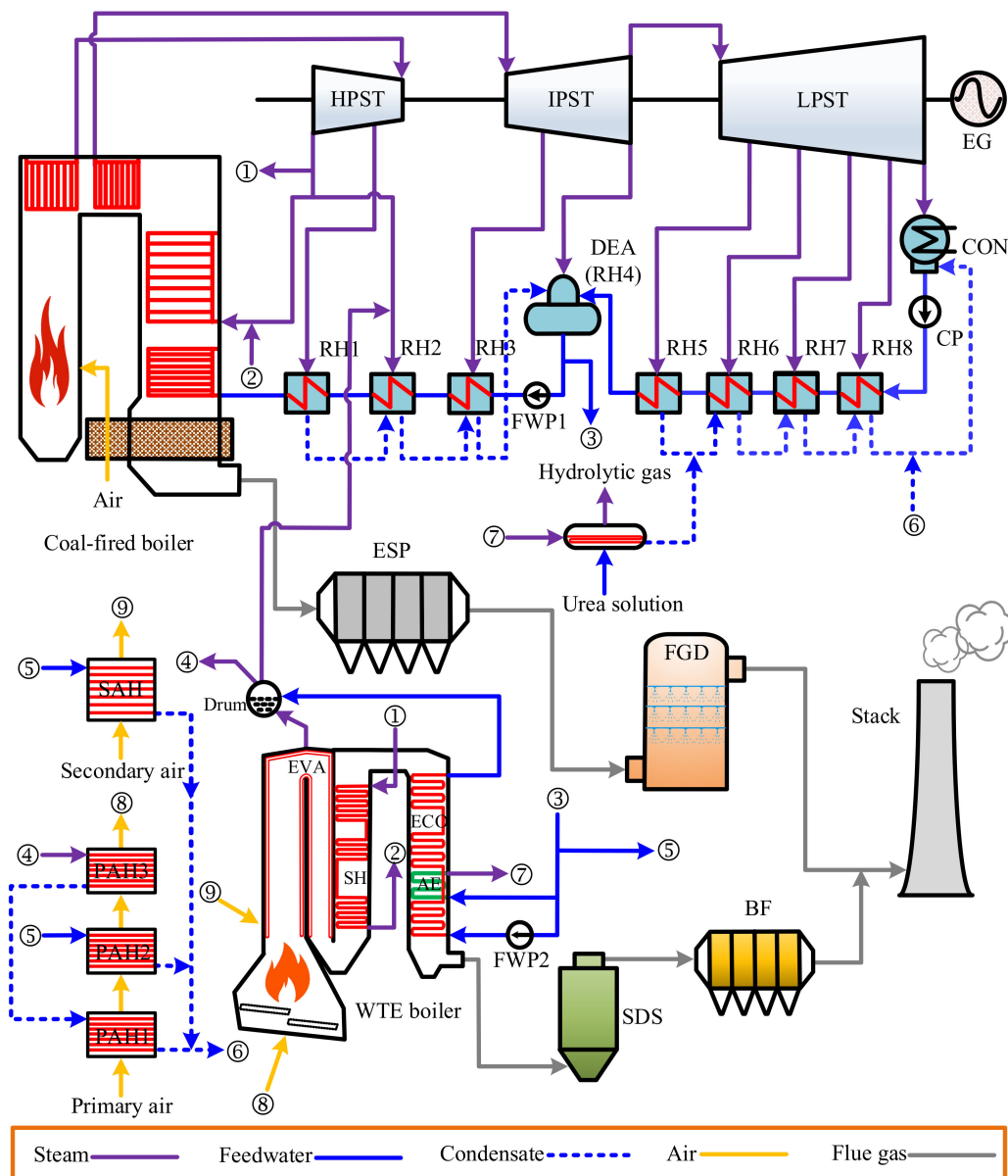

Figure 3. Diagram of the proposed integration design.

In general, the available energy from MSW combustion is transferred to the steam–water cycle of CFPU by integrating with the CFPU system, contributing to a remarkable augmentation in total electricity generation. Meanwhile, several facilities of the WTEU are removed, saving a large number of investment and operation costs.

4. Modeling

4.1. Essential Assumptions

The advantages of integrated design are identified under the 100% load of reference power systems. Several critical assumptions need to be stated for stand-alone and integrated designs to validate the feasibility of proposed scheme.

1. The temperature of exhaust flue gas in the WTE boiler and its thermal efficiency are constant [31].
2. The thermal efficiency of CFPU boiler and its auxiliary power are invariant [31].
3. The consumption rates of coal and MSW are unchanged [31].
4. The power generated by coal combustion keeps invariable [31].
5. The power generation of the WTE system is considered variable [31].
6. The ambient pressure and temperature are 1 atm and 15.0 °C, respectively.

4.2. Initial System Modeling

EBSILON Professional is applied to simulate the initial and proposed systems, which is universally employed in modeling thermodynamic systems. The models of WTE system, coal-fired system and integrated power generation system are established based on the original data of reference power plants, as illustrated in Appendix A (Figure A1). Simulation results of these systems are certified by their design data under 100% rated output load. The data comparisons between initial and proposed designs are separately exposed in Tables 8 and 9. The simulated values are very close to the design values, indicating models are accurate and reliable.

Table 8. Comparison between the simulation and design values of WTEU under 100% rated output load.

Comparison		Unit	Design	Simulation	Relative Error (%)
Fuel consumption rate		kg/s	5.79	5.79	0.00
Live steam	Pressure	MPa	4.10	4.10	0.00
	Temperature	°C	400.0	400.0	0.00
	Mass flow	kg/s	13.50	13.50	0.00
Exhaust steam	Pressure	MPa	0.007	0.007	0.00
	Temperature	°C	39.0	39.0	0.00
	Mass flow	kg/s	9.95	9.96	0.10
Exhaust gas temperature		°C	190.0	189.9	−0.05
Total power generation		MW	9.74	9.75	0.10
Net power generation		MW	7.99	8.00	0.13

Table 9. Comparison between the simulation and design values of CFPU under 100% rated output load.

Comparison		Unit	Design	Simulation	Relative Error (%)
Fuel consumption rate		kg/s	59.72	59.72	0.00
Live steam	Pressure	MPa	24.20	24.20	0.00
	Temperature	°C	566.0	566.0	0.00
	Mass flow	kg/s	506.35	506.35	0.00
Reheat steam	Pressure	MPa	3.82	3.82	0.00
	Temperature	°C	566	566	0.00
	Mass flow	kg/s	432.42	432.31	−0.03
Exhaust steam	Pressure	MPa	0.0049	0.0049	0.00
	Temperature	°C	32.5	32.5	0.00
	Mass flow	kg/s	322.83	322.17	−0.20
Total power generation		MW	659.34	659.57	0.03
Net power generation		MW	626.37	626.59	0.04

4.3. Integrated System Modeling

The simulation and calculation achieve the data of proposed integrated design in EBSILON professional. Due to the removal of several devices of WTEU, the parameters of working fluid entering and leaving the WTE system have changed a lot compared to the stand-alone WTEU. The AE is arranged in the ECO space of the WTE boiler. The cold side inlet fluid extracts from the feedwater of WTEU, absorbs the flue gas heat and turns into saturated steam at specific pressure and temperature. The ammonia produced by urea hydrolysis is used to remove the NOx in coal-fired boiler. Now, the heat source (the third stage extraction steam of the STs of CFPU) for UHU is replaced by the saturated steam generated from the AE of WTE boiler. The outlet steam of AE gets into UHU to transfer heat to the urea solution, and the condensate flows into the RH6 with the drain water of RH5. The steam source used in the urea hydrolyzer is changed from the original high-temperature steam to the saturated steam produced by AE. The steam pressure reduced from the original 2.13 MPa to 1.01 MPa and its temperature decreased from 473.9 °C to 180.5 °C. At the same time, the saturated steam no longer needs to be sprayed demineralized water to reduce its temperature and pressure, which can significantly improve the safety of hydrolyzer. In addition, regardless of the type of coal entering the boiler, according to the changes in NO_x concentration during the operation, the mass flow of steam required by the urea hydrolysis device can be directly adjusted for the ammonia production, which improves the operation flexibility of hydrolyzer. The critical parameters of AE are displayed in Table 10, and the comparison of UHU in initial and integrated designs is exhibited in Table 11.

Table 10. Parameters of the AE in the integrated design.

	Parameter	Unit	Value
Cold side	Inlet/outlet fluid	-	Feedwater/saturated steam
	Inlet/outlet pressure	MPa	1.09/1.01
	Inlet/outlet temperature	°C	180.3/180.5
	Mass flow	kg/s	0.72
Hot side	Inlet/outlet fluid	-	Flue gas/flue gas
	Inlet/outlet temperature	°C	271.3/235.5
	Mass flow	kg/s	35.61
	LMTD	°C	71.6
	Heat load	MW	1.45

Table 11. Comparison of the UHU in the initial and integrated designs.

	Parameter	Unit	Initial Design	Integrated Design
Cold side	Inlet/outlet fluid	-	Urea solution/ Hydrolytic gas	Urea solution/ Hydrolytic gas
	Inlet/outlet temperature	°C	50.0/150.0	50.0/150.0
	Mass flow	kg/s	0.67	0.67
Hot side	Steam pressure	MPa	2.13	1.01
	Steam temperature	°C	473.9	180.5
	Steam flow	kg/s	0.58	0.72
	Attempering water pressure	MPa	1.10	-
	Attempering water temperature	°C	25.0	-
	Attempering water flow	kg/s	0.14	-
	LMTD	°C	76.9	77.5
	Heat load	MW	1.41	1.41

The SH and ECO of WTE boiler are separately applied to heat partial cold reheat steam from CFPU and the feedwater of WTEU in the hybrid design. The parameters of SH and ECO are shown in Table 12. The boiler efficiency is invariant when the MSW consumption rate and exhaust flue gas temperature behind ECO keep fixed. The 30.76 kg/s cold reheat steam is heated in the SH of WTE boiler, causing an increase from 308.4 °C to 400.0 °C in steam temperature, and then absorbing heat in the RHR of CFPU. The 14.12 kg/s feedwater from CFPU enters the ECO of WTE boiler and is increased from 181.0 °C to 254.4 °C. The LMTD of SH and ECO is dropped after the system combination, leading to their heat transfer area expansion.

Table 12. Comparison of the ECO and SH between the initial and integrated designs.

Comparison		Unit	Initial Design		Integrated Design	
			ECO	SH	ECO	SH
Cold side	Inlet/outlet fluid	-	Feedwater/ feedwater	Saturated steam/ superheated steam	Feedwater/ feedwater	Superheated steam/ superheated steam
	Inlet/outlet pressure	MPa	5.30/4.50	4.50/4.10	5.30/4.50	4.24/4.04
	Inlet/outlet temperature	°C	130.1/254.4	257.4/400.0	181.0/254.4	308.4/400.0
	Mass flow	kg/s	14.19	13.50	14.12	30.76
Hot side	Inlet/outlet fluid	-	Flue gas/ flue gas	Flue gas/ flue gas	Flue gas/ flue gas	Flue gas/ flue gas
	Inlet/outlet temperature	°C	382.7/189.9	513.5/382.7	342.3/189.9	513.6/342.3
	Mass flow	kg/s	35.61	35.61	35.61	35.61
	LMTD	°C	89.7	119.3	34.50	65.9
	Heat load	MW	7.91	5.60	4.76	7.29

The heat source of PAH1 and PAH3 in hybrid design remains unchanged, while that of PAH2 and SAH alters from the extraction steam of ST to the feedwater from the DEA of CFPU. The outlet air parameters of each section of APHs remain invariant. Thus, their parameters (cold side) are dismissed. The parameters of APHs in the new WTE system are described in Table 13. Since the working fluid mass flow of PAH1 and PAH3 varies, their operation state is changed. The variation in the heat transfer condition of APHs results in their LMTD reducing and area increasing. The mass flow variation of each extraction steam stage (stage 1–8) of CFPU before and after system combination is exhibited in Figure 4. With the system integration, the saturated steam from WTE boiler drum is transported to the extraction steam of RH2 of CFPU. Therefore, the second stage extraction steam flow reduces, and the power output increases.

Table 13. Variation in the APHs of WTEU in the integrated design.

Parameter		Unit	PAH1	PAH2	PAH3	SAH
Hot side	Inlet/outlet fluid	-	Condensate/ condensate	Feedwater/ condensate	Steam/ condensate	Feedwater/ condensate
	Inlet/outlet pressure	MPa	4.30/3.90	1.09/0.99	4.50/4.30	1.09/0.99
	Inlet/outlet temperature	°C	178.5/37.7	180.3/32.4	257.4/178.5	180.3/22.2
	Mass flow	kg/s	0.56	4.45	0.56	1.91
	LMTD	°C	66.7	5.4	22.7	10.4
	Heat load	MW	0.33	2.79	1.13	1.28

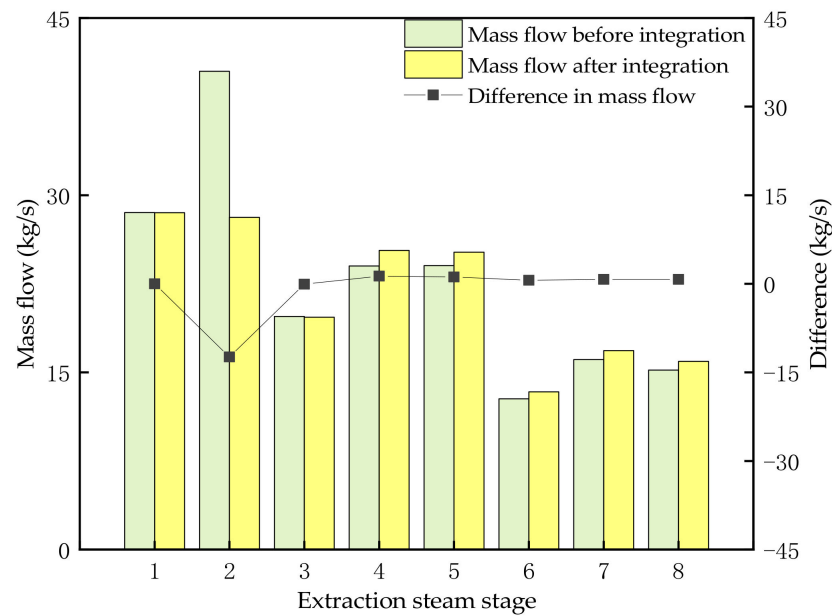**Figure 4.** Variation in the mass flow of each extraction steam stage of CFPU before and after system integration.

5. Thermodynamic Evaluation

5.1. Energy Analysis and Results

The energy performances of stand-alone and integrated designs are compared under 100% rated output load, where the extra power generation is examined by an equal fuel consumption rate. The net power generation of WTEU in the integrated design is defined as ($P_{w,int}$):

$$P_{w,int} = P_{tot,int} - P_c \tag{4}$$

where $P_{tot,int}$ is the net total power generation of integrated design, MW; P_c is the net power generation of CFPU, MW, considered invariant in both designs.

The net waste-to-energy efficiency ($\eta_{en,w}$) and the net total energy efficiency ($\eta_{en,tot}$) are expressed as:

$$\eta_{en,w} = \frac{P_w}{m_w \times q_w} \tag{5}$$

$$\eta_{en,tot} = \frac{P_{tot}}{m_c \times q_c + m_w \times q_w} \tag{6}$$

where P_w is the net power generation of WTE system, MW; P_{tot} is the net total power generation of two systems, MW; m_w and m_c are consumption rates of MSW and coal, kg/s; q_w and q_c are net calorific values of MSW and coal, kJ/kg.

The energy analysis results of initial and proposed designs are depicted in Table 14. As the coal-fired and WTE systems are combined, not only does the mass flow of reheat steam entering the CFPU boiler increase, but the work output of STs augments as well. In addition, the consumption rates of coal and MSW keep constant. As a result, the gross power generation is increased by 3.91 MW. Moreover, the total auxiliary power is decreased by 0.33 MW because of several devices' removals in the proposed WTE design, including condensate pump (CP) and circulating water pump (CWP). Accordingly, the net total power generation of hybrid system is improved by 4.25 MW, increasing the net total energy efficiency from 41.84% to 42.12%. Considering the power generation of CFPU is invariant, the net power generation of WTE system is raised from 8.00 to 12.25 MW, increasing the net waste-to-energy efficiency from 19.73% to 30.21%. Energy analysis results expose that the proposed design improves the thermal efficiency of WTE system.

Table 14. Comparison of the energy analysis results between the initial and proposed designs.

	Parameter	Initial Design	Proposed Design	Difference
WTEU	MSW consumption rate (kg/s)	5.79	5.79	0
	Live steam mass flow (kg/s)	13.50	-	-
	Exhaust steam mass flow (kg/s)	9.96	-	-
	Boiler efficiency (%)	78.55	78.55	0
CFPU	Coal consumption rate (kg/s)	59.72	59.72	0
	Live steam mass flow (kg/s)	506.35	506.21	−0.14
	Reheat steam mass flow (kg/s)	432.31	444.56	+12.25
	Exhaust steam mass flow (kg/s)	322.17	330.52	+8.35
	Boiler efficiency (%)	93.22	93.22	0
	Total power generation (MW)	669.32	673.23	+3.91
	Total auxiliary power (MW)	34.73	34.40	−0.33
	Net total power generation (MW)	634.59	638.83	+4.25
	Net power generation of WTEU (MW)	8.00	12.25	+4.25
	Net waste-to-energy efficiency (%)	19.73	30.21	+10.48
	Net total energy efficiency (%)	41.84	42.12	+0.28

5.2. Energy Flow Diagram

The energy flow occurring in the initial and integrated designs is investigated to explore the cause for the performance improvement of recommended integration, as exhibited in Figure 5. The energy flow in combined system differs from that of two separate systems because the energy transfer or conversion between two units is conducted by different heat exchangers. In the two designs, the total energy input of fuel remains invariable and is considered as 100%. The energy values and corresponding proportions transmitted in each process of systems are also shown in the diagrams. In the incorporated system, 37.94 MW and 7.29 MW of heat from the WTE boiler are transferred to the steam–water cycle of CFPU. Simultaneously, 4.07 MW and 11.42 MW of energy from the STs of CFPU are transmitted to the WTE system. The total power output and energy efficiency are enhanced by 3.91 MW and 0.28% after combination. Compared with the stand-alone design, the total exhaust steam flow reduces by 1.61 kg/s (according to Table 14), and the total exhaust steam energy loss drops by 3.90 MW in the proposed design. The total power output increment is very close to the energy loss reduction of exhaust steam in the CON of CFPU, which validates the decrease in total exhaust steam mass flow is the prime reason for power generation increment.

5.3. Exergy Analysis and Results

Exergy analysis could find the prime location and quantity of irreversible losses in thermodynamic systems and propose methods to improve the whole system's performance. The exergy of fuel (EX_f, MW) is calculated as follows [31].
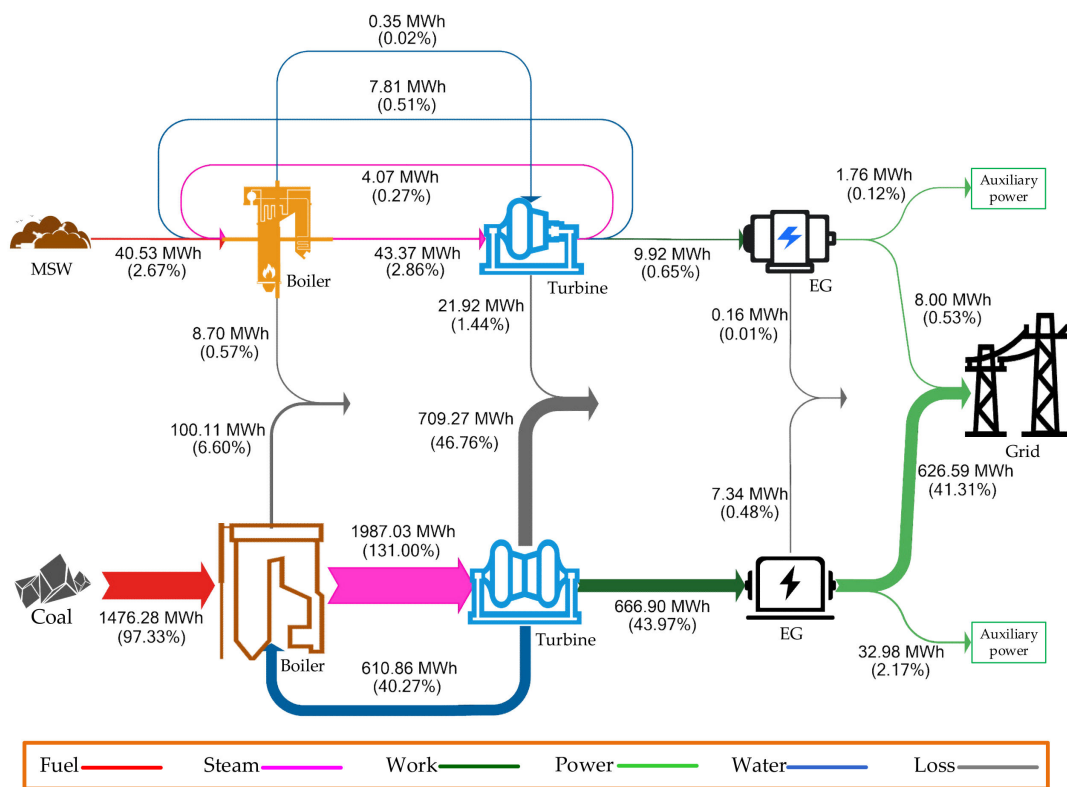
$$EX_f = m_f \times q_f \times (1.0064 + 0.1519 \frac{w(H)}{w(C)} + 0.0616 \frac{w(O)}{w(C)} + 0.0429 \frac{w(N)}{w(C)}) \qquad (7)$$

where m_f is the fuel consumption rate, kg/s; q_f is the net calorific values of fuel, kJ/kg; $w(C)$, $w(H)$ $w(O)$ and $w(N)$ are the mass contents of hydrogen, carbon, oxygen and nitrogen in fuels.
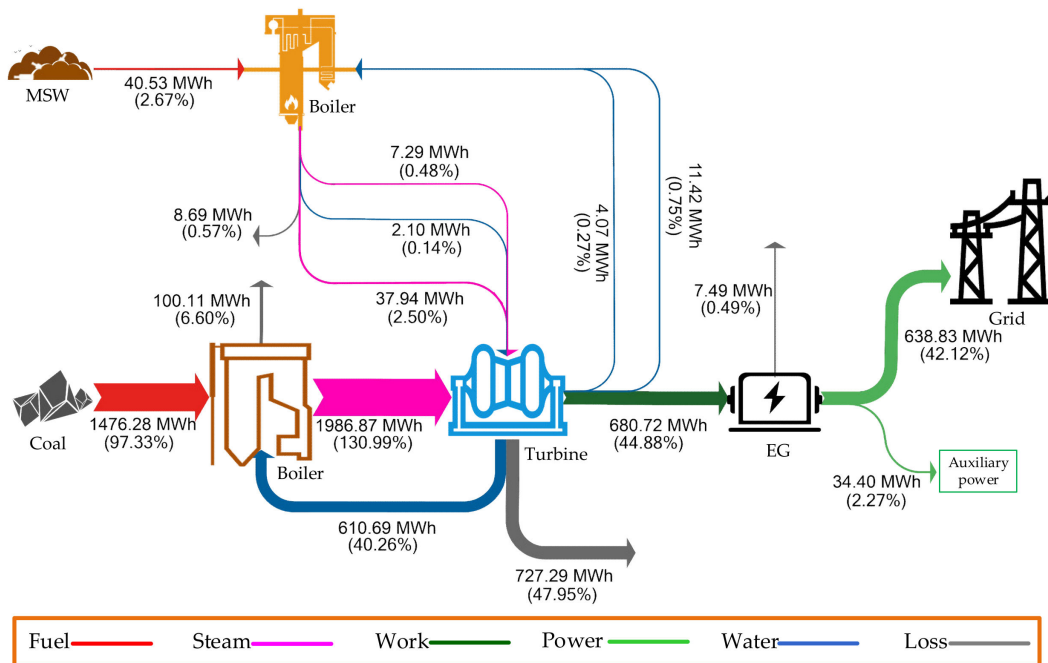
The exergy of a fluid (EX_{fd}, MW) is expressed as [26]:

$$EX_{fd} = m_{fd} \times [h - h_0 - T_0 \times (s - s_0)] \qquad (8)$$

where m_{fd} is the mass flow of a fluid, kg/s; T_0 is the ambient temperature, K; h and h_0 are the enthalpy of a fluid at the current and environmental states, kJ/kg; s and s_0 are the entropy of a fluid at the current and environmental states, kJ/(kg·K). The ambient temperature and pressure are 15 °C and 1 atm.

(**a**)

(**b**)

Figure 5. Energy flow diagrams of the initial and proposed designs. (**a**) Initial design; (**b**) proposed design.

The exergy efficiency of WTE system ($\eta_{\text{ex,w}}$) and the total exergy efficiency of proposed system ($\eta_{\text{ex,tot}}$) are defined as:

$$\eta_{\text{ex,w}} = \frac{P_{\text{w}}}{EX_{\text{w}}} \tag{9}$$

$$\eta_{\text{ex,tot}} = \frac{P_{\text{tot}}}{EX_{\text{w}} + EX_{\text{c}}} \tag{10}$$

where EX_{w} is the exergy of MSW, MW; EX_{c} is the exergy of coal, MW.

Contrastive analysis between the initial and suggested systems is carried out to explore the energy synergism of combined design, and Table 15 summarizes the results. The exergy loss variation of major equipment is illustrated in Figure 6, and the following points deserve attention before and after system integration.

Table 15. Comparison of the exergy analysis results between the initial and proposed designs.

Parameter		Initial Design		Proposed Design		Difference
		MW	**Proportion**	**MW**	**Proportion**	**MW**
Exergy input of CFPU		1497.95	97.22%	1497.95	97.22%	0.00
Exergy input of WTEU		42.82	2.78%	42.82	2.78%	0.00
Total exergy input		1540.76	100.00%	1540.76	100.00%	0.00
Net exergy output of CFPU		626.59	40.67%	626.59	40.67%	0.00
Net exergy output of WTEU		8.00	0.52%	12.25	0.79%	+4.25
Net total exergy output		634.59	41.19%	638.83	41.46%	+4.25
Exergy loss variation						
CFPU	Boiler	720.09	46.74%	719.71	46.71%	−0.38
	Turbine	45.94	2.98%	46.82	3.04%	+0.88
	RHs	14.84	0.96%	15.22	0.99%	+0.38
	CON	40.60	2.63%	41.61	2.70%	+1.02
	EG	7.34	0.48%	7.49	0.49%	+0.15
	UHU	0.66	0.04%	0.51	0.03%	−0.14
	Auxiliary power	32.98	2.14%	32.98	2.14%	0.00
	Other	8.92	0.58%	8.97	0.58%	+0.05
WTEU	Boiler	26.20	1.70%	25.68	1.67%	−0.52
	Turbine	2.66	0.17%	-	-	−2.66
	RHs + APHs	2.33	0.15%	1.52	0.10%	−0.81
	CON	1.72	0.11%	-	-	−1.72
	EG	0.16	0.01%	-	-	−0.16
	Auxiliary power	1.76	0.11%	1.42	0.09%	−0.34
Total exergy loss		906.18	58.81%	901.93	58.54%	−4.25
Net total exergy efficiency			41.19%		41.46%	0.28%
Net exergy efficiency of WTEU			18.68%		28.60%	+9.92%

1. The exergy loss in WTE boiler is declined by 0.52 MW, because heat transfer temperature difference of those heat exchangers in WTE boiler diminishes. The exergy loss in CFPU boiler is decreased by 0.38 MW, primarily triggered by the cold reheat steam temperature increase. As a result, the total boiler exergy loss is reduced by 0.89 MW.

2. The exergy loss in all STs is shrunk by 1.78 MW with sharing a higher efficiency and larger scale steam turbine generator set.

3. As the saturated steam from WTE boiler drum is sent to the extraction steam pipe of RH2, the exergy loss of RHs of CFPU increased by 0.38 MW. At the same time, in WTEU, because the RH is removed, the heat sources of SAH and PAH2 are replaced, the working fluid mass flow of PAH3 and PAH1 is adjusted, and the heat transfer temperature difference of each section of APHs is reduced, the exergy of RHs and APHs is decreased by 0.81 MW. Therefore, the total exergy loss of RHs and APHs of integrated system is reduced by 0.43 MW.

4. The total exhaust steam flow of STs falls, which contributes to the CON exergy loss reducing by 0.70 MW.
5. The exergy loss in UHU is decreased by 0.15 MW, with the heat source of UHU varying after combination.
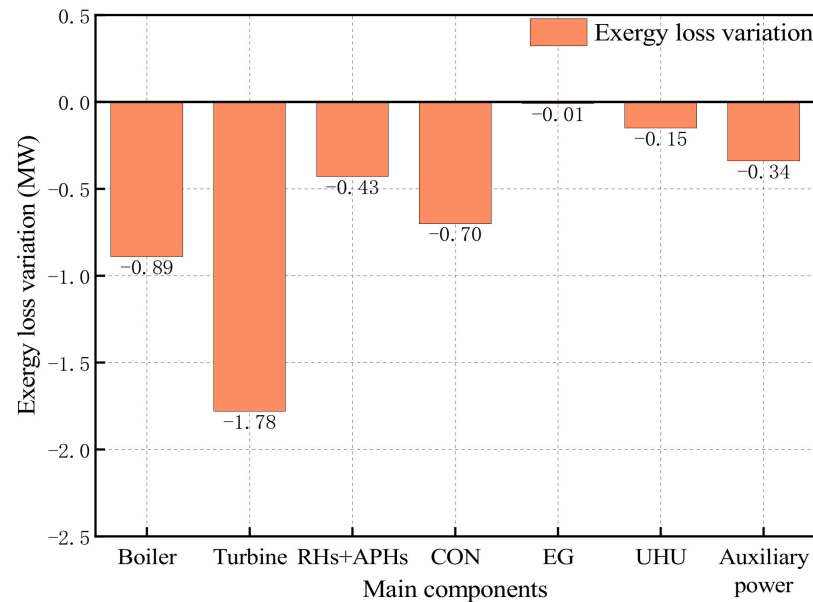6. There is no apparent change in the exergy loss of other components.

Figure 6. Exergy loss variation of several main components after system integration.

In summary, the overall exergy destruction of systems is reduced by 4.25 MW after integration. The exergy efficiency of WTE system is increased by 9.92%, and 0.28% improvement in total exergy efficiency is achieved compared to the initial systems. Exergy analysis results show that the primary reason for efficiency growth is the exergy loss reduction in turbines and boilers, while most energy change occurs in CON through energy analysis.

6. Economic Evaluation

Economic evaluation of the novel WTE design is required to examine the financial feasibility of integrated design. In separate and integrated designs, the costs and benefits of CFPU are considered unchanged, and the economic benefit of WTE system is investigated independently. When the WTEU employs domestic equipment, its investment cost is 52,975 $/t [40]. The proposed WTE project is considered a 25-year build–operate–transfer project, including two years for building and twenty-three years for capital recovery. The incomes of WTE plants rely on electricity sales and waste disposal. The Chinese government usually determines the on-grid tariff and waste disposal subsidy [41]. The essential data of economic analysis is provided in Table 16.

In the proposed WTE design, several components are changed in comparison with the initial WTEU. The cost of altered equipment is assessed by the scale-up method and estimation function. The expenses of equipment (such as turbine, pump and EG) are determined by estimation functions. The charges of devices (including PAH, SAH and SH) are calculated by the scale-up method, as depicted in Equation (11) [31]. The primary data of estimation function and scale-up method are described in Tables 17 and 18.

$$C_{\text{ch}} = C_{\text{ref}} \times \left(\frac{S_{\text{ch}}}{S_{\text{ref}}}\right)^f \tag{11}$$

where C_{ch} and S_{ch} denote the capital costs ($) and scale parameters of changed equipment in the present scale; C_{ref} and S_{ref} are the reference capital cost ($) and reference scale parameters of transformed equipment in the basic scale; f is the scale factor.

Table 16. Essential parameters of the economic analysis.

Parameter		Unit	Value	Source
Total investment of proposed WTEU		M$	26.49	[40]
Yearly operation and maintenance cost of WTEU		M$	10% of total investment cost	[31]
Yearly operating time of WTEU		h	7000	
Project period	Building period	year	2	[42]
	Payback period	year	23	
Discount rate		-	8%	[42]
Waste disposal subsidy		$/t	13.04	[40]
On-grid power tariff		$/MWh	99.97	[43]
Income tax rate	1st to 3rd year	%	0	[41]
	4th to 6th year	%	12.5	
	7th to 25th year	%	25.0	

M$: million USD.

Table 17. Estimation function for the cost of partial components.

Component	Function	Source
Turbine	$IC_{\text{T}} = 6000 \times (W_T)^{0.71}$	[44]
EG	$IC_{\text{EG}} = 60 \times (P_{EG})^{0.95}$	[45]
CP, EP, FWP and CWP	$IC_{\text{P}} = 3540 \times (W_P)^{0.71}$	[44]
RH2	$\log_{10}(IC_{\text{HX}}) = 4.8306 - 0.8509 \times \log_{10}(A) + 0.3187 \times \left[\log_{10}(A)\right]^2$	[46]
DEA	$IC_{\text{DEA}} = 6014 \times (m_{\text{fw}})^{0.7}$	[45]
AE	$IC_{AE} = 130 \times \left(\frac{A_{AE}}{0.093}\right)^{0.78}$	[44]

Table 18. Primary data of the scale-up method for the cost of several facilities.

Facility	Basic Cost (k$)	Basic Scale	Unit	Scale Factor	Source
Cooling tower	27,355.45	1,845,000	m^2	1	
CON	1715.287	18,000	m^2	1	[47]
Stack	3827.12	1,178,352	m^3/h	1	
SH	45.84	500	m^2	0.741	[48]
ECO	693.00	13,149	m^2	0.68	[49]
PAH	800.00	8372	m^2	0.68	[50]
SAH	800.00	8372	m^2	0.68	

The total cost of new WTE system is affected by the changed equipment. The expenses of changed components are displayed in Table 19. Some equipment (ST, EG, CON, etc.) of the hybrid WTE system are removed, saving about $6.07 million. Several devices (ECO, SAH, PAH and SH) are transformed in the integrated design, resulting in an increased cost of $0.72 million. Furthermore, an extra cost of $0.07 million is produced because of the employment of several components such as EP and AE. Consequently, the total cost of proposed WTE system is decreased by around $5.15 million after the system combination.

Table 19. Comparison of the investment cost between initial and proposed WTE designs.

Component		Initial WTE Design (k$)	Proposed WTE Design (k$)	Difference (k$)
Removed	ST	4126.61	-	−4126.61
	EG	369.71	-	−369.71
	CON	45.53	-	−45.53
	CWP	211.74	-	−211.74
	Cooling tower	920.06	-	−920.06
	CP	8.90	-	−8.90
	RH2	18.96	-	−18.96
	DEA	38.51	-	−38.51
	Stack	331.86	-	−331.86
Transformed	ECO	246.58	346.08	+99.50
	SH	107.78	203.60	+95.82
	PAH	252.53	761.37	+508.84
	SAH	109.58	257.31	+147.73
Added	EP	-	7.09	+7.09
	AE	-	62.88	+62.88
Sum		6788.35	1638.33	−5150.03

The total investment of proposed WTE design ($C_{tot,pw}$, $) is calculated by Equation (12).

$$C_{tot,pw} = C_{tot,ow} - \sum C_{cc} \tag{12}$$

where $C_{tot,ow}$ is the total investment of original WTEU, $; $\sum C_{cc}$ is the total investment of changed components, $.

The dynamic payback period (DPP, year) and the net present value (NPV, $) are evaluated to examine the economic benefits of proposed WTE design. DPP is calculated by the project's net cash flow each year after discounting it into the present value at a specific discount rate [51]. The DPP is determined by Formula (13), and a shorter DPP means faster payback. The NPV denotes the present value of net profit in the whole project life cycle, which is defined by Equation (14) [42]. More NPV reveals the more profitable the project is.

$$\sum_{a=1}^{DPP} \frac{C_{in} - C_{out}}{(1 + r_{dis})^a} = 0 \tag{13}$$

$$NPV = \sum_{a=1}^{n} \frac{(C_{in} - C_{out})}{(1 + r_{dis})^a} \tag{14}$$

where a is a year in the lifetime of a project; C_{in} and C_{out} represent the cash inflows and outflows in a year, $; r_{dis} is the discount rate; n is the project lifetime, year.

During the construction of suggested WTE project, it is not profitable. In the economic period, the yearly cash inflows depend on the income from electricity sales and waste disposal, which can be expressed as:

$$C_{in} = P_w \times t \times c_e + m_w \times 3.6 \times t \times c_{wds} \tag{15}$$

where t is the operating hours of WTEU in a year, h; c_e is the on-grid tariff, $/kWh; c_{wds} is the waste disposal subsidy, $/t.

In the building period, the investment cost of suggested WTE project is cash outflows. In the payback period, the income tax and the cost of operation and maintenance are the cash outflows. The cash outflow (C_{out}) of WTE project is conveyed as:

$$C_{out} = C_{it} + C_{o\&m} \tag{16}$$

$$C_{it} = [C_{in} - C_{o\&m}] \times r_{it} \tag{17}$$

where C_{it} is the annual income tax, \$, obtained by Formula (17); $C_{o\&m}$ is the operation and maintenance cost per year, \$; C_{in} is the gross annual income, \$; r_{it} is the income tax rate.

The above formulas evaluate the economy of initial and proposed WTE projects, and the results are presented in Table 20. The annual operating time of proposed WTEU is reduced by 1500 h compared to the original case, leading to a decline in MSW disposal volumes, and the yearly waste disposal income is decreased from \$1.90 million to \$1.49 million. The net power generation of WTEU is risen by 4.25 MW under 100% load, contributing to an increase of 11.38 GWh in the annual power output and an increment in the annual power supply revenue from \$5.60 million to \$6.75 million. The total cost of proposed WTE system is dropped by \$5.15 million, and its annual operation and maintenance costs are cut by \$0.52 million. In addition, over the whole life cycle of integrated WTE system, the DPP falls from 11.39 years to 5.48 years and the NPV reaches \$24.02 million and achieves an increase of \$14.42 million, compared to the initial WTE system. Detailed calculations of NPV and DPP are presented in the Supplementary Materials.

Table 20. Comparison of economic analysis results between the initial and proposed WTE designs.

Comparison	Unit	Initial WTE Design	Proposed WTE Design	Difference
Total investment	M\$	26.49	21.34	−5.15
MSW consumption per year	t	145833	114583	−31,250
Annual waste disposal income	M\$	1.90	1.49	−0.41
Net power generation	MW	8.00	12.25	+4.25
Net annual power generation (the 100% load of CFPU is 5500 h per year)	GWh	56.00	67.38	+11.38
Annual electricity sales income	M\$	5.60	6.74	+1.14
Total annual income	M\$	7.50	8.23	+0.73
Yearly operation and maintenance cost	M\$	2.65	2.13	−0.52
Dynamic payback period	year	11.39	5.48	−5.91
Net present value	M\$	9.60	24.02	+14.42

7. Discussion

The integration method is what researchers need to consider when coupling different thermal systems. According to previous research on the integration of a coal-fired power plant and a waste incineration power plant [31,33], aiming for the net power output of integrated system, the net power output results are compared under several integrated modes as follows:

(a)   Mode 1: Directly apply the scheme of Reference [31];
(b)   Mode 2: Modify APHs based on reference WTEU and Mode 1;
(c)   Mode 3: Transport the outlet superheated steam of SH of WTEU to the RHR of CFPU based on Mode 1;
(d)   Mode 4: Directly adopt the scheme of Reference [33];
(e)   Mode 5: Change the outlet steam of SH of WTE boiler to RHR of CFPU based on Mode 4;
(f)   Mode 6: Modify APHs based on Mode 5;
(g)   Mode 7: Integrated scheme in this paper.

Among the above seven modes, the method of APHs transformation is the same. The net power output results are presented in the Figure 7. As shown from Figure 7, the net power output of the integrated design in this paper (Mode 7) is the largest, that of Mode 1 is the second, and that of Mode 4 is the least. However, compared with the total net power output of 634.59 MW under the stand-alone designs, whichever integrated scheme can obtain a significant increase in power output. Therefore, integrated design is worthy of popularization and application.
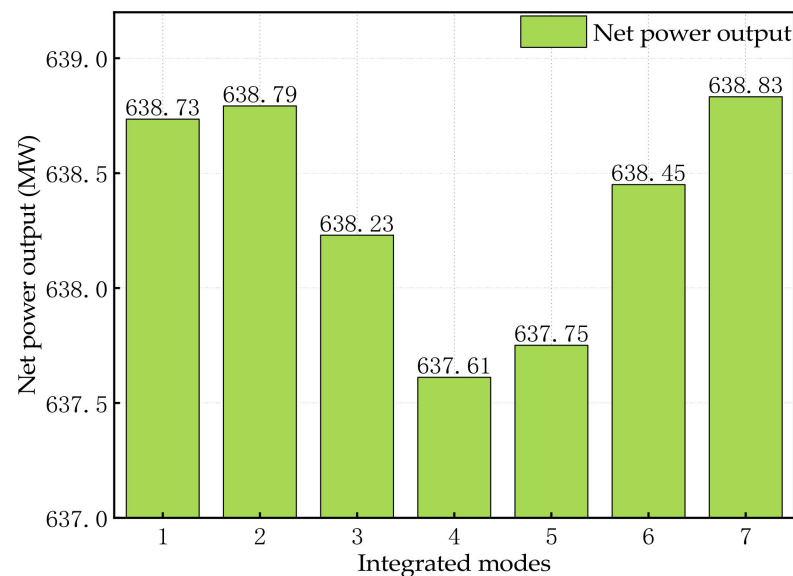
Figure 7. The net power output result of different integrated modes.

The previous works [31,33] have improved net power output effectively. Comparing the results of Mode 1 and Mode 2, it is not difficult to find that the net power output can be increased slightly when adopting the transformation of APHs. Therefore, the transformation of APHs is active. Comparing the results of Mode 1 and Mode 3, it is found that directly feeding the outlet steam of SH of WTE boiler to the RHR of CFPU boiler can also improve the overall net power output. Still, the effect is not as good as the Mode 1, therefore, using the SH of WTE boiler to heat the exhaust steam of HPST is better than using that to heat drum steam. Comparing the results of Mode 4 and Mode 5, it is more effective for net power output improvement to deliver the superheated steam from SH of WTE boiler to RHR of CFPU boiler in Mode 5. Based on Mode 5, the APHs are modified, and the net power generation is further increased, proving that the modification of APHs is valid. Comparing the results of Mode 1 and Mode 4, the integration design of Mode 1 is more favorable than that of Mode 4. Finally, after contrasting the results of Mode1 to Mode 6, the integration design in this article (Mode 7) is proposed and achieves the best net power output result. The flowcharts of these modes are depicted in Supplementary Materials.

8. Conclusions

An integrated WTE system based on the steam–water cycle and urea hydrolysis process of a CFPU is developed to improve the performance of WTEU, according to the previous works. In the integrated design, partial cold reheat steam of CFPU absorbs the energy from WTE boiler. Simultaneously, the heat required for partial preheated air of WTEU and its feedwater are supplied by the feedwater of CFPU. Furthermore, the heat source for the UHU is varied from the extraction steam of STs of CFPU to the outlet stream of AE in WTE boiler. The results demonstrate that the integrated WTE system could generate more electricity and a remarkable boost in its energy efficiency. Based on a 500 t/d WTEU and a 660 MW CFPU, the conventional stand-alone units and the suggested system are evaluated by thermodynamics and economics methods. In addition, the net power outputs of different integration modes are compared based on the two units. The main results are concluded as follows:

1. When consumption rates of coal and MSW keep unchanged, the WTE system in the new configuration can generate an extra 4.25 MW of net power output and increase power generation efficiency by 10.48%. The reduction of energy loss in CON could explain the upturn in power generation of the proposed design through energy analysis.

2. System integration reduces the exergy loss of boilers, STs and CON by 0.89 MW, 1.78 MW and 0.70 MW, with the decrease of heat transfer temperature difference

in boilers and the reduction of the total exhaust steam flow in STs. Subsequently, the exergy efficiency of WTEU is raised by 9.92%, and the total exergy efficiency of suggested system is enhanced by 0.28%.

3. After the system integration, the DDP of WTE system is cut down from 11.39 years to 5.48 years. Its NPV is augmented from $9.60 million to $24.02 million, confirming the financial feasibility of the innovative hybrid design.

4. According to the comparison of listed integration modes, the mode with the highest net power generation is adopted in this paper. Among the compared modes, the utilized way of SH of WTE boiler has become the main factor affecting the total power output difference of the integrated system. In addition, exergy analysis results indicate that the larger heat transfer temperature difference will cause more exergy loss, reducing net power output. That's why the outlet fluid from each heat exchanger of WTEU must be mixed with the working fluid at a close temperature in the CFPU to maximize the energy output.

Author Contributions: Conceptualization, Y.Z. and H.C.; methodology, H.C.; software, L.W.; validation, Y.Z., H.C. and K.Z.; formal analysis, Y.Z.; investigation, L.W.; resources, Q.L.; data curation, X.G.; writing—original draft preparation, Y.Z.; writing—review and editing, Q.H.; visualization, L.W.; supervision, H.C.; project administration, Q.L.; funding acquisition, H.C. All authors have read and agreed to the published version of the manuscript.

Institutional Review Board Statement: Not applicable.

Informed Consent Statement: Not applicable.

Data Availability Statement: Data are contained within the article.

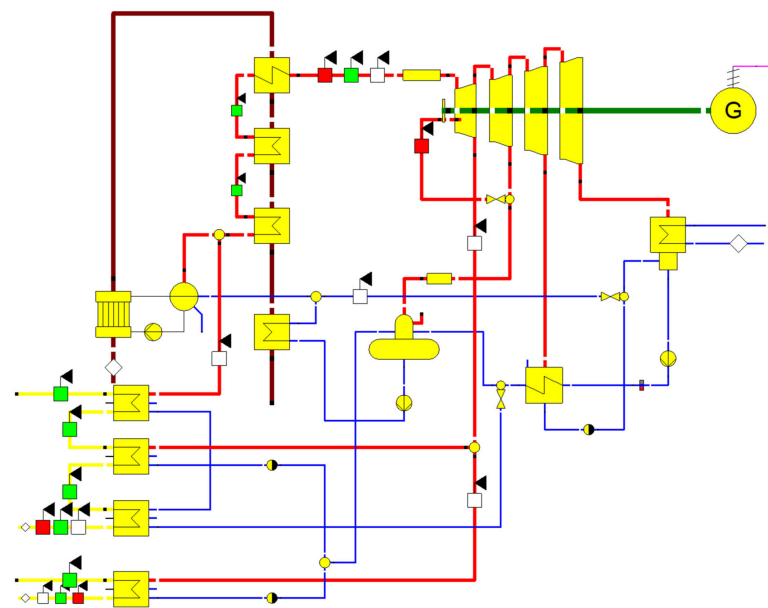**Conflicts of Interest:** The authors declare no conflict of interest.

Nomenclature

Abbreviation

AE	additional evaporator	IPST	intermediate-pressure steam turbine
APH	air preheater	LMTD	logarithmic mean temperature difference
BF	bag filter	LPST	low-pressure steam turbine
CFPU	Coal-fired power unit	MSW	municipal solid waste
CON	condenser	NPV	net present value
CP	condensate pump	PAH	primary air heater
CWP	circulating water pump	RH	regenerative heater
DEA	deaerator	RHR	reheater
DPP	dynamic payback period	SAH	secondary air heater
ECO	economizer	SCR	selective catalytic reduction
EG	electricity generator	SDS	semi-dry scrubber
EP	extra pump	SH	superheater
ESP	electrostatic precipitator	ST	steam turbine
EVA	evaporator	UHU	urea hydrolysis unit
FGD	flue gas desulfurization	WTE	waste-to-energy
FWP	feedwater pump	WTEU	waste-to-energy unit
HPST	high-pressure steam turbine		

Symbol

A	area (m^2)	NO	nitric oxide
a	a year in project lifetime	NO_2	nitrogen dioxide
C	carbon/cost (\$)/cash flow (\$)	NOx	nitrogen oxides
$CO(NH_2)_2$	urea	n	mole ratio (%)/project lifetime (year)
c	cash flow (\$)	O	oxygen
Cl	chlorine	P	power (kW)
EX	exergy (kW)	ΔQ	concerntration change (mg/m^3)
f	scale factor	q	net calorific value (kJ/kg)
H	hydrogen	r	rate (%)
h	enthalpy (kJ/kg)	S	sulfur/scale parameter
η	efficiency (%)	s	entropy (kJ/(kg·K))
IC	investment cost (\$)	t	yearly operation time (h)
M	molar mass (g/mol)	T	temperature (K)
$M\$$	Million USD	V	volume (Nm^3/h)
m	mass flow (kg/s)	W	work (kW)
N	nitrogen	w	weight (%)
NH_3	ammonia		

subscript

0	ambient state	HX	heat exchanger
AE	additional evaporator	in	inlet/inflow
c	coal	int	integrated
cc	changed components	it	income tax (\$)
ch	changed	out	outlet/outflow
DEA	deaerator	$o\&m$	operation and maintenance
dis	discount	ow	original WTEU
EG	electricity generator	P	pump
e	electricity (kWh)	pw	proposed WTEU
en	energy (kW)	ref	reference
ex	exergy (kW)	T	turbine
f	fuel	tot	total
fd	fluid	w	waste
fw	feedwater	wds	waste disposal subsidy

Appendix A. Simulation Models of the Reference Power Systems

(a)
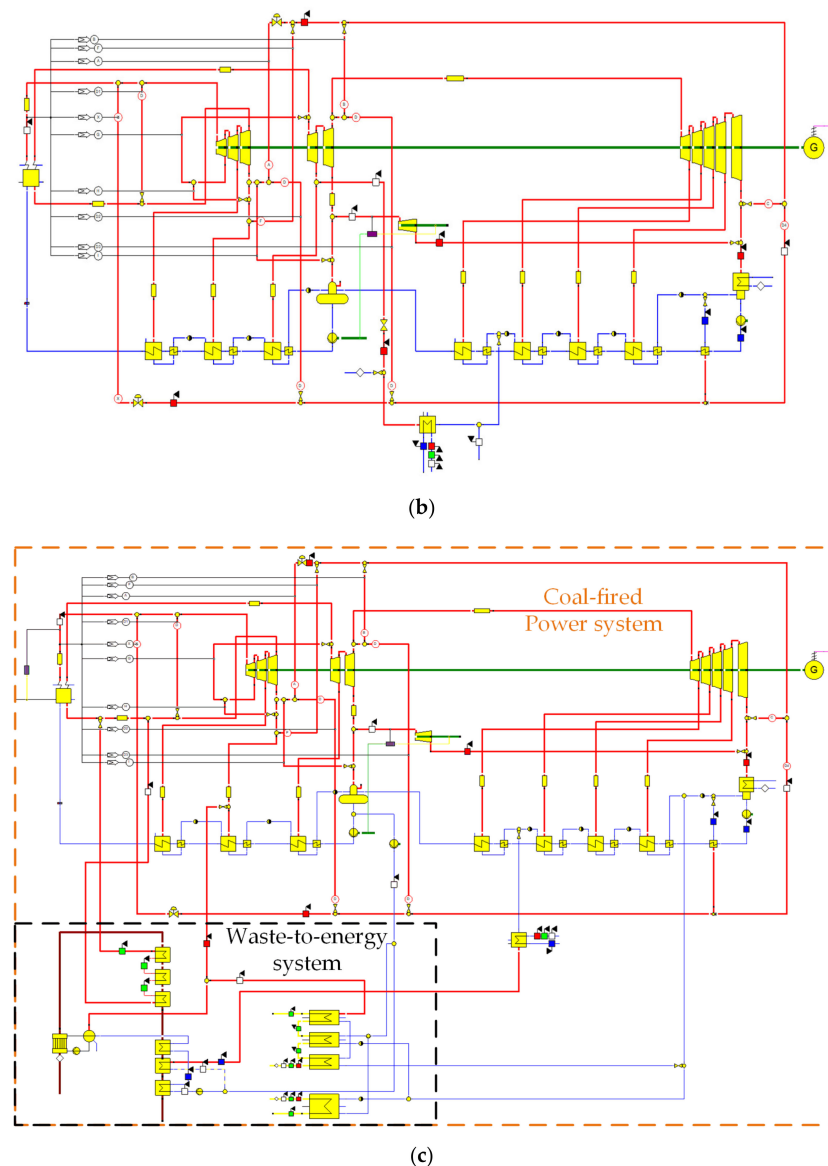
Figure A1. *Cont.*

(**b**)

(**c**)

Figure A1. Models of the researched power generation systems in EBSILON Professional. (**a**) Model of the reference WTEU; (**b**) model of the reference CFPU; (**c**) model of the integrated power generation system.

References

1. Sun, C.; Meng, X.; Peng, S. Effects of waste-to-energy plants on china's urbanization: Evidence from a hedonic price analysis in Shenzhen. *Sustainability* **2017**, *9*, 475. [CrossRef]
2. Ji, L.; Lu, S.; Yang, J.; Du, C.; Chen, Z.; Buekens, A.; Yan, J. Municipal solid waste incineration in China and the issue of acidification: A Review. *Waste Manag. Res. J. A Sustain. Circ. Econ.* **2016**, *34*, 280–297. [CrossRef] [PubMed]
3. National Bureau of Statistics. Municipal Solid Waste Removal and Disposal. Available online: https://data.stats.gov.cn (accessed on 25 August 2021).
4. Xu, H.; Lin, W.Y.; Dal Magro, F.; Li, T.; Py, X.; Romagnoli, A. Towards higher energy efficiency in future waste-to-energy plants with novel latent heat storage-based thermal buffer system. *Renew. Sustain. Energy Rev.* **2019**, *112*, 324–337. [CrossRef]
5. Tun, M.M.; Palacky, P.; Juchelková, D.; Síťař, V. Renewable waste-to-energy in southeast Asia: Status, challenges, opportunities, and selection of waste-to-energy technologies. *Appl. Sci.* **2020**, *10*, 7312. [CrossRef]
6. Fei, F.; Wen, Z.; Huang, S.; De Clercq, D. Mechanical biological treatment of municipal solid waste: Energy efficiency, environmental impact and economic feasibility analysis. *J. Clean. Prod.* **2018**, *178*, 731–739. [CrossRef]
7. Cesaro, A.; Belgiorno, V. Anaerobic Digestion of Mechanically Sorted Organic Waste: The influence of storage time on the energetic potential. *Sustain. Chem. Pharm.* **2021**, *20*, 100373. [CrossRef]

8. Leme, M.M.V.; Rocha, M.H.; Lora, E.E.S.; Venturini, O.J.; Lopes, B.M.; Ferreira, C.H. Techno-economic analysis and environmental impact assessment of energy recovery from municipal solid waste (MSW) in Brazil. *Resour. Conserv. Recycl.* **2014**, *87*, 8–20. [CrossRef]

9. Li, Y.; Zhao, X.; Li, Y.; Li, X. Waste incineration industry and development policies in China. *Waste Manag.* **2015**, *46*, 234–241. [CrossRef]

10. Mian, M.M.; Zeng, X.; Nasry, A.A.N.B.; Al-Hamadani, S.M.Z.F. Municipal solid waste management in China: A comparative analysis. *J. Mater. Cycles Waste Manag.* **2017**, *19*, 1127–1135. [CrossRef]

11. Makarichi, L.; Jutidamrongphan, W.; Techato, K. The evolution of waste-to-energy incineration: A review. *Renew. Sustain. Energy Rev.* **2018**, *91*, 812–821. [CrossRef]

12. Lombardi, L.; Carnevale, E.; Corti, A. A review of technologies and performances of thermal treatment systems for energy recovery from waste. *Waste Manag.* **2015**, *37*, 26–44. [CrossRef] [PubMed]

13. Müller, D.; Wöllmer, S.; Aßbichler, D.; Murer, M.J.; Heuss-Aßbichler, S.; Rieger, K.; Hill, H.; Härtel, C.; Masset, P.J. High temperature corrosion studies of a zirconia coating: Implications for waste-to-energy (WTE) plants. *Coatings* **2016**, *6*, 36. [CrossRef]

14. Lee, S.; Themelis, N.J.; Castaldi, M.J. High-temperature corrosion in waste-to-energy boilers. *J. Therm. Spray Technol.* **2007**, *16*, 104–110. [CrossRef]

15. Martin, J.J.E.; Koralewska, R.; Wohlleben, A. Advanced solutions in combustion-based WtE technologies. *Waste Manag.* **2015**, *37*, 147–156. [CrossRef] [PubMed]

16. Koralewska, R. Innovative concepts of high-efficiency EfW plants. In Proceedings of the 16th Annual North American Waste-to-Energy Conference, Philadelphia, PA, USA, 19–21 May 2008.

17. Bogale, W.; Viganò, F. A preliminary comparative performance evaluation of highly efficient waste-to-energy plants. *Energy Procedia* **2014**, *45*, 1315–1324. [CrossRef]

18. Liuzzo, G.; Verdone, N.; Bravi, M. The benefits of flue gas recirculation in waste incineration. *Waste Manag.* **2007**, *27*, 106–116. [CrossRef] [PubMed]

19. Strobel, R.; Waldner, M.H.; Gablinger, H. Highly efficient combustion with low excess air in a modern energy-from-waste (EfW) plant. *Waste Manag.* **2018**, *73*, 301–306. [CrossRef]

20. Stehlík, P. Up-to-date technologies in waste to energy field. *Rev. Chem. Eng.* **2012**, *28*, 223–242. [CrossRef]

21. Alrobaian, A.A. Improving waste incineration CHP plant efficiency by waste heat recovery for feedwater preheating process: Energy, exergy, and economic (3E) analysis. *J. Braz. Soc. Mech. Sci. Eng.* **2020**, *42*, 403. [CrossRef]

22. Arabkoohsar, A.; Nami, H. Thermodynamic and economic analyses of a hybrid waste-driven CHP–ORC plant with exhaust heat recovery. *Energy Convers. Manag.* **2019**, *187*, 512–522. [CrossRef]

23. Zuo, W.; Zhang, X.; Li, Y. Review of flue gas acid dew-point and related low temperature corrosion. *J. Energy Inst.* **2020**, *93*, 1666–1677. [CrossRef]

24. De Greef, J.; Villani, K.; Goethals, J.; Van Belle, H.; Van Caneghem, J.; Vandecasteele, C. Optimising energy recovery and use of chemicals, resources and materials in modern waste-to-energy plants. *Waste Manag.* **2013**, *33*, 2416–2424. [CrossRef] [PubMed]

25. Chen, X.; Xue, X.; Si, Y.; Liu, C.; Chen, L.; Guo, Y.; Mei, S. Thermodynamic analysis of a hybrid trigenerative compressed air energy storage system with solar thermal energy. *Entropy* **2020**, *22*, 764. [CrossRef]

26. Pan, P.; Wu, Y.; Chen, H. Performance evaluation of an improved biomass-fired cogeneration system simultaneously using Extraction Steam, Cooling Water, and Feedwater for Heating. *Front. Energy* **2021**, 1–15. [CrossRef]

27. Hulgaard, T.; Sondergaard, I. Integrating waste-to-energy in Copenhagen, Denmark. *Proc. Inst. Civ. Eng. Civ. Eng.* **2018**, *171*, 3–10. [CrossRef]

28. Nami, H.; Arabkoohsar, A.; Anvari-Moghaddam, A. Thermodynamic and sustainability analysis of a municipal waste-driven combined cooling, heating and power (CCHP) plant. *Energy Convers. Manag.* **2019**, *201*, 112158. [CrossRef]

29. Bianchi, M.; Branchini, L.; De Pascale, A. Combining waste-to-energy steam cycle with gas turbine units. *Appl. Energy* **2014**, *130*, 764–773. [CrossRef]

30. Mendecka, B.; Lombardi, L.; Gładysz, P.; Stanek, W. Exergo-ecological assessment of waste to energy plants supported by solar energy. *Energies* **2018**, *11*, 773. [CrossRef]

31. Chen, H.; Zhang, M.; Xue, K.; Xu, G.; Yang, Y.; Wang, Z.; Liu, W.; Liu, T. An innovative waste-to-energy system integrated with a coal-fired power plant. *Energy* **2020**, *194*, 116893. [CrossRef]

32. Sun, L.; Wu, C. Theory and practice of ammonia production by hydrolysis of urea for flue gas denitration. *Clean Coal Technol.* **2020**, *26*, 229–236. (In Chinese)

33. Chen, H.; Zhang, M.; Chen, Z.; Xu, G.; Han, W.; Liu, W.; Liu, T. Performance analysis and operation strategy of an improved waste-to-energy system incorporated with a coal-fired power unit based on feedwater heating. *Appl. Therm. Eng.* **2020**, *178*, 115637. [CrossRef]

34. Carneiro, M.L.N.M.; Gomes, M.S.P. Energy, exergy, environmental and economic analysis of hybrid waste-to-energy plants. *Energy Convers. Manag.* **2019**, *179*, 397–417. [CrossRef]

35. Lu, F.; Zhu, Y.; Pan, M.; Li, C.; Yin, J.; Huang, F. Thermodynamic, economic, and environmental analysis of new combined power and space cooling system for waste heat recovery in waste-to-energy plant. *Energy Convers. Manag.* **2020**, *226*, 113511. [CrossRef]

36. STEAG Energy Services. EBSILON Professional Documentation. Available online: https://www.ebsilon.com/en/ (accessed on 22 November 2021).

37. Costa, M.; Indrizzi, V.; Massarotti, N.; Mauro, A. Modeling and optimization of an incinerator plant for the reduction of the environmental impact. *Int. J. Numer. Methods Heat Fluid Flow* **2015**, *25*, 1463–1487. [CrossRef]

38. Wang, X.; Li, W.; Wang, N.; Bai, C.; Xiao, H. Mechanism and influence factors of ammonia production using urea. *Therm. Power Gener.* **2019**, *48*, 101–107. (In Chinese)

39. Feng, M.; Yan, H. Research on the concentration value conversion of NO_x in the flue gas from thermal power plants. *Shanxi Electr. Power* **2007**, *103*, 15–16. (In Chinese)

40. Zhao, X.; Jiang, G.; Li, A.; Wang, L. Economic analysis of waste-to-energy industry in China. *Waste Manag.* **2016**, *48*, 604–618. [CrossRef] [PubMed]

41. Zeng, X. Cost Analysis of waste incineration-power generation projects. *Environ. Sanit. Eng.* **2014**, *22*, 57–60. (In Chinese)

42. Li, C.; Wang, F.; Zhang, D.; Ye, X. Cost management for waste to energy systems using life cycle costing approach: A case study from China. *J. Renew. Sustain. Energy* **2016**, *8*, 25901. [CrossRef]

43. National Development and Reform Commission. Notice of the National Development and Reform Commission on Improving the Price Policy of Waste Incineration for Power Generation. 2021. Available online: www.ndrc.gov.cn (accessed on 29 August 2021).

44. Ogorure, O.J.; Oko, C.O.C.; Diemuodeke, E.O.; Owebor, K. Energy, exergy, environmental and economic analysis of an agricultural waste-to-energy integrated multigeneration thermal power plant. *Energy Convers. Manag.* **2018**, *171*, 222–240. [CrossRef]

45. Lian, Z.T.; Chua, K.J.; Chou, S.K. A thermoeconomic analysis of biomass energy for trigeneration. *Appl. Energy* **2010**, *87*, 84–95. [CrossRef]

46. Zhang, C.; Liu, C.; Wang, S.; Xu, X.; Li, Q. Thermo-economic comparison of subcritical organic Rankine cycle based on different heat exchanger configurations. *Energy* **2017**, *123*, 728–741. [CrossRef]

47. Electric Power Planning and Engineering Institute. *Quota Design Reference Cost Indicators for Thermal Power Projects*; 2016 Edition; China Electric Power Press: Beijing, China, 2017. Available online: https://www.doc88.com/p-9943837447835.html (accessed on 22 November 2021).

48. Elsido, C.; Martelli, E.; Kreutz, T. Heat integration and heat recovery steam cycle optimization for a low-carbon lignite/biomass-to-jet fuel demonstration project. *Appl. Energy* **2019**, *239*, 1322–1342. [CrossRef]

49. Xu, G.; Xu, C.; Yang, Y.; Fang, Y.; Li, Y.; Song, X. A novel flue gas waste heat recovery system for coal-fired ultra-supercritical Power Plants. *Appl. Therm. Eng.* **2014**, *67*, 240–249. [CrossRef]

50. Xu, C.; Xu, G.; Han, Y.; Liang, F.; Fang, Y.; Yang, Y. A novel lignite pre-drying system with low-grade heat integration for modern lignite power plants. *Chin. Sci. Bull.* **2014**, *59*, 4426–4435. [CrossRef]

51. Mi, X.; Liu, R.; Cui, H.; Memon, S.A.; Xing, F.; Lo, Y. Energy and economic analysis of building integrated with PCM in different cities of China. *Appl. Energy* **2016**, *175*, 324–336. [CrossRef]